Tropospheric aqueous-phase oxidation of green leaf volatiles with $^{\bullet}OH$ and $SO_4^{\bullet-}$ and $NO_3^{\bullet}$ radicals

Kumar Sarang[1*], Tobias Otto[3], Krzysztof Rudzinski[1], Irena Grgić[2] , Klara Nestorowicz[1], Hartmut Herrmann[3] and Rafal Szmigielski[1*]

Contact info: ksarang@ichf.edu.pl, ralf@ichf.edu.pl

[1]Institute of Physical Chemistry, Polish Academy of Sciences, Warsaw, Poland
[2]Department of Analytical Chemistry, National Institute of Chemistry, Ljubljana, Slovenia
[3]Atmospheric Chemistry Department, Leibniz Institute for Tropospheric Research, Leipzig, Germany

1 Introduction

Numerous green leaf volatiles (GLVs) are released into the atmosphere due to the stress, cell damage or wounding.[1]

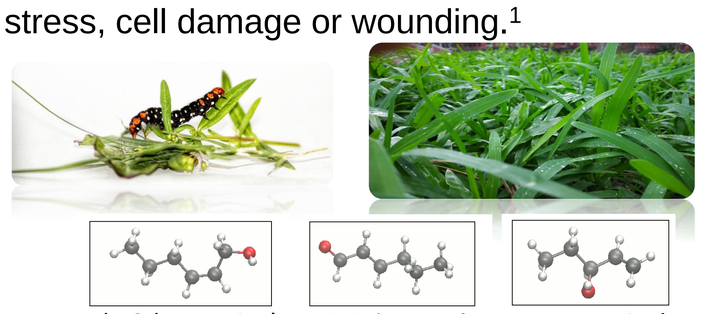

cis-2-hexen-1-ol | 2-E-hexenal | 1-penten-3-ol

Secondary Organic Aerosol (SOA) formation through aqueous-phase reaction of GLV

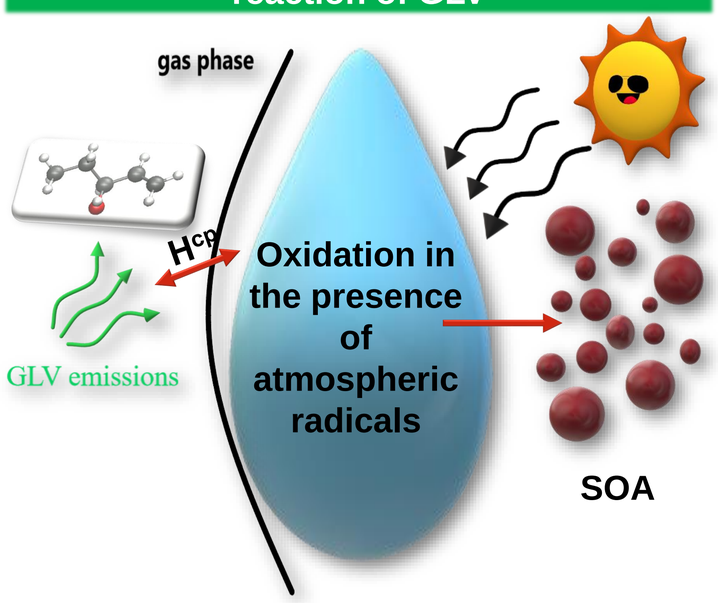

Motivation

- Kinetic investigations of GLVs in the gas phase have already been reported[2,3], while there is no kinetic data on the aqueous phase reactions of selected C6 and C5 GLVs.
- Significant gap in our knowledge of SOA through aqueous-phase processes.
- GLVs as a source of SOA is still poorly recognized.
- In the present study, we focussed on the kinetic studies of GLVs with $^{\bullet}OH$, $SO_4^{\bullet-}$ and $NO_3^{\bullet}$ radicals as a possible source of aqueous SOA.

2 Experimental method

Kinetic setup

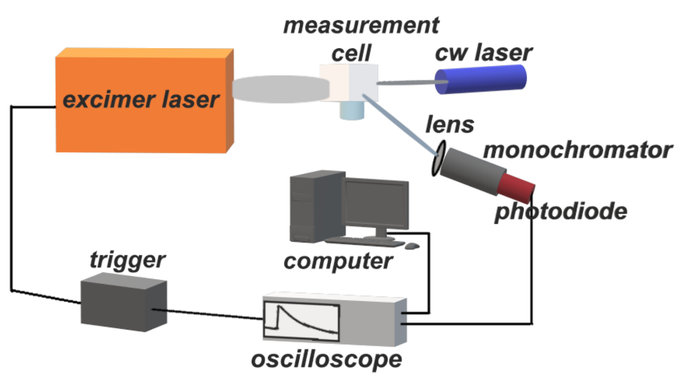

Figure 1: Laser flash photolysis-laser long path absorption (LFP-LLPA) setup similar to previous studies[5]

Table 1: Experimental conditions

Radical	Precursors (mol L^{-1})	Excimer laser (nm)	CW laser (nm)	Measurement
$^{\bullet}OH$	$[H_2O_2]$ = 2 x 10^{-4} [KSCN] = 2 x 10^{-5}	248, 308	407, 473	competition
$SO_4^{\bullet-}$	$[S_2O_8^{2-}]$ = 5 x 10^{-4}	248, 308	407, 473	direct
$NO_3^{\bullet}$	$[S_2O_8^{2-}]$= 0.03 $[NO_3]$ = 0.1	351	635	direct

Competition kinetics[4]

$^{\bullet}OH$ + GLV → Products		**R1**
$^{\bullet}OH$ + SCN^- ⇋ $SCNOH^{\bullet-}$		**R2**
$SCNOH^{\bullet-}$ ⇋ $SCN^{\bullet}$ + OH^-		**R3**
$SCN^{\bullet}$ + SCN^- ⇋ $(SCN)_2^{\bullet-}$		**R4**

k_{2nd} is the second order rate constant of **R 1**
k_{ref} is the overall second order rate constant of **R 2-4**,

$$\frac{A_{[(SCN)_2^-]_0}}{A_{[(SCN)_2^-]_X}} = \frac{k_{2nd}[GLV]}{k_{ref}[SCN^-]} + 1 \quad (1)$$

(Schaefer and Herrmann, 2018)

$$k_{ref}(T) = e^{(28.87)-1690/T} L\ mol^{-1} s^{-1} \quad (2)$$

(Zhu, Nicovich et al. 2003)

3 Results

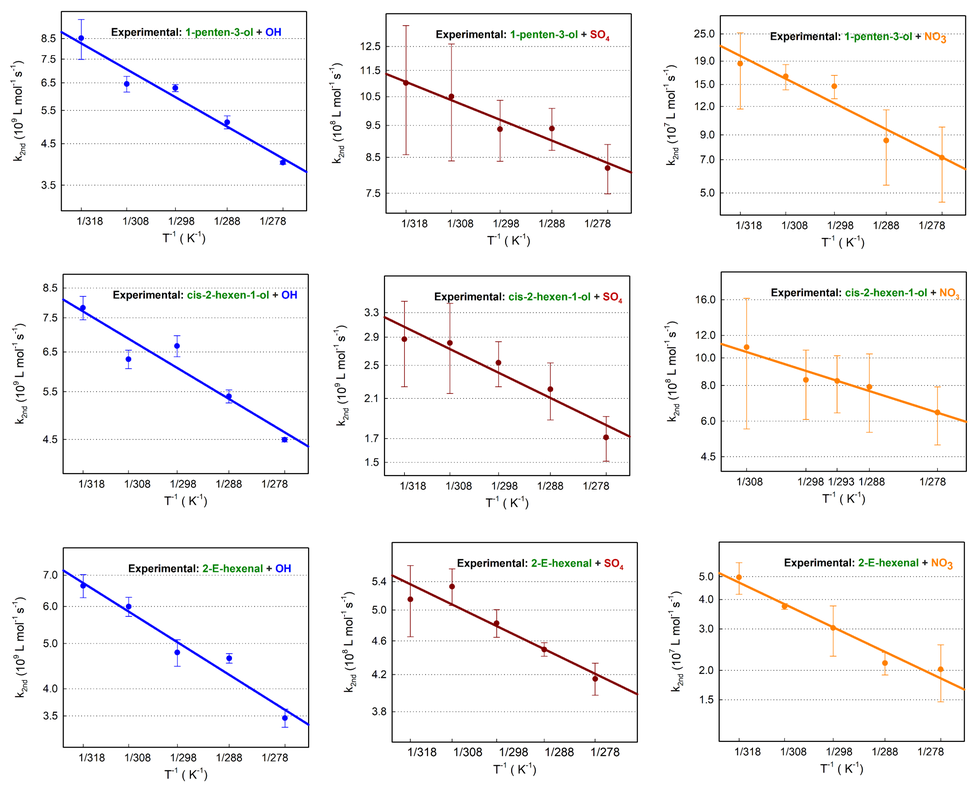

Figure 2: Arrhenius plots depicting temperature dependence of the reaction of 1-penten-3-ol, cis-2-hexen-1-ol and 2-E-hexanal with $^{\bullet}OH$, $SO_4^{\bullet-}$ and $NO_3^{\bullet}$ respectively

- Arrhenius plot shows the weak temperature dependence of the aqueous-phase reactions of GLVs.
- Experimental rate constant is considerably fast (order 10^7-10^9).

Table 2: Experimentally observed rate constants for reactions of GLVs with $^{\bullet}OH$, $SO_4^{\bullet-}$ and $NO_3^{\bullet}$ at 298 K.

GLV	Radical	k_{obs} 10^8 L mol^{-1} s^{-1}
P-3-ol	$^{\bullet}OH$	63.0 ± 1.4
Hex-1-ol		66.6 ± 3.0
2-Hexal		47.8 ± 3.1
P-3-ol	$SO_4^{\bullet-}$	9.4 ± 1.0
Hex-1-ol		25.3 ± 3.0
2-Hexal		4.8 ± 0.2
P-3-ol	$NO_3^{\bullet}$	1.5 ± 0.2
Hex-1-ol		8.4 ± 2.3
2-Hexal		0.3 ± 0.1

4 Conclusions

- Temperature dependent kinetic investigation of GLVs (1-penten-3-ol, cis-2-hexen-1-ol and 2-E-hexanal) with $^{\bullet}OH$, $SO_4^{\bullet-}$ and $NO_3^{\bullet}$
- Reactivity order of GLVs : $^{\bullet}OH$ > $SO_4^{\bullet-}$ > $NO_3^{\bullet}$
- Higher is the rate constant, higher is the percentage diffusion and lower is the calculated activation energy.

Table 5: Activation parameters calculated using Arrhenius equation determined

Radical	GLV	$E_A/kJ\ mol^{-1}$	$A/L\ mol^{-1}\ s^{-1}$	$\Delta H^{\ddagger}\ kJ\ mol^{-1}$	$\Delta S^{\ddagger}\ J\ mol^{-1}K^{-1}$	$\Delta G^{\ddagger}\ kJ\ mol^{-1}$
$SO_4^{\bullet-}$	P-3-oL	5.19 ± 0.78	$(7.86 \pm 0.13) \times 10^9$	2.71 ± 0.50	−63.80 ± −1.09	21.70 ± 4.40
	Hex-1-ol	9.50 ± 1.61	$(1.11 \pm 0.03) \times 10^{11}$	7.02 ± 1.47	−41.70 ± −1.33	19.50 ± 4.71
	2-Hexal	4.45 ± 0.88	$(2.89 \pm 0.06) \times 10^9$	1.97 ± 0.48	−72.10 ± −1.46	23.50 ± 6.20
$^{\bullet}OH$	P-3-oL	12.80 ± 1.54	$(1.04 \pm 0.03) \times 10^{12}$	10.30 ± 1.54	−23.20 ± −0.65	17.20 ± 3.06
	Hex-1-ol	9.41 ± 1.77	$(2.47 \pm 0.08) \times 10^{11}$	6.94 ± 1.62	-35.10 ± −1.19	17.40 ± 4.66
	2-Hexal	11.20 ± 1.54	$(4.31 \pm 0.12) \times 10^{11}$	8.74 ± 1.49	−30.50 ± −0.88	17.80 ± 3.55
$NO_3^{\bullet}$	P-3-oL	18.90 ± 2.97	$(2.50 \pm 0.14) \times 10^{11}$	16.40 ± 3.20	−35.00 ± −1.99	26.80 ± 6.76
	Hex-1-ol	11.6 ± 1.64	$(9.88 \pm 0.327) \times 10^{10}$	9.16 ± 1.60	−42.7 ± −1.41	21.9 ± 4.56
	2-Hexal	17.20 ± 2.03	$(3.16 \pm 0.13) \times 10^{10}$	14.70 ± 2.16	−52.20 ± −2.20	30.30 ± 5.71

5 Atmospheric implications

- Aqueous-phase reactions were investigated for lifetimes in deliquescent, haze and cloud water.
- Order of aqueous-phase lifetime follows the order of increase in liquid water content, and hence, maximum in deliquescent water and minimum in cloud water ranging from several days to single minutes.

References

[1] Fisher, A. J., Grimes, H. D., & Fall, R. (2003). Phytochemistry.. [2] Shalamzari et al, (2014) Environ. Sci. Technol. [3] Davis, M. E., & Burkholder, J. B. (2011). Atmos. Chem. Phys. [4] Behar, D., Bevan, P. L. T., & Scholes, G. (1972). J. Phys. Chem. [5] Otto, T., Stieger, B., Mettke, P., & Herrmann, H. (2017). J. Phys. Chem. A, 121, 6460-6470. [6] Schaefer and Herrmann, Phys. Chem. Chem. Phys., 2018. [7] L. Zhu, J. M. Nicovich and P. H. Wine, Aquatic Sciences, 2003.

Acknowledgement

ERASMUS + mobility programme